

# A Carbon Nanotube-Based Sensor for Measuring Forces at the Cellular Scale

C. Roman, F. Ciontu, B. Courtois

TIMA Laboratory, 46. Av. Félix Viallet, 38031 Grenoble, France,  
{cosmin.roman, florin.ciontu, bernard.courtois}@imag.fr

## ABSTRACT

In this paper we perform a theoretical study of a potential design for a carbon-nanotube device able to transduce forces developed at the scale of basic cellular processes into current variations. The proposed device transduces the deflection of a carbon nanotube upon the application of an external perturbation into a variation of the currents at the ends of a second nanotube, perpendicular to the former. The first stage of this study consists of an assessment of the sensitivity of the devices with forces in the tens of pNs, developed typically at the cellular scale. In the second stage, we focus on the transduction of the deflection of the cantilever into an electrical signal.

**Keywords:** carbon nanotubes, nano-mechanical cantilever, biosensors, molecular modeling,

## 1 INTRODUCTION

The last few years have brought nanotech applications closer to the realm of reality mainly due to considerable progress in fabricating nanostructures with controlled properties. Carbon nanotubes followed this path with huge advances in synthesis techniques as well as functionalization [1], solubility and selection [2]. Given this trend it is reasonable to extrapolate that in several years there is a possibility of having nanotubes with well controlled properties at significantly lower costs. Aside from this, an essential aspect that allows envisioning the design of carbon-nanotube based structures is the very good correlation between theoretical models and experimental data.

Bio-sensing is one application domain offering some clear opportunities to transpose scientific advances related to nanotubes into applications.

In this paper we theoretically investigate a potential design for a carbon-nanotube device able to transduce forces developed at the scale of basic cellular processes into current variations.

Measuring cell forces is one possible application for this device. Also, compared to microscopic cantilevers carbon nanotube based devices would have the advantage of a far better scale compatibility with the elementary biological processes. The scale compatibility is the first of the four requirements for the future generation of bio-sensors, followed by the need for label-free detection, scalability to allow massive parallelization and sensitivity of detection range.

The remainder of the paper is structured as follows. In Section 2 we explain the functioning principle of the sensor. Section 3 contains the details on the calculations performed to characterize the mechanics of the sensor. The transduction of mechanical movement into a current variation is presented in Section 4. Finally, we present our conclusions in Section 5.

## 2 FORCE SENSOR OPERATION PRINCIPLE

The proposed device transduces the deflection of a carbon nanotube upon the application of an external perturbation into a variation of the currents at the ends of a second nanotube, perpendicular to the former.

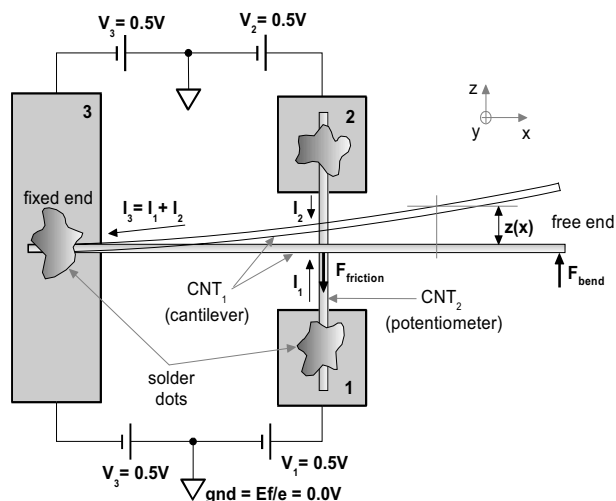


Figure 1: Schematic representation of the principle of operation of a carbon nanotube-based force sensor, including electronic biasing.

The schematic of the device is depicted in Figure 1. The transversal tube is locked down at both its ends while the longitudinal tube is fixed at one end and free standing at the other. A deformation force will elastically bend the cantilever, shifting the position of the cross-junction along the former tube. If the tubes are electrically biased with the aid of some metallic leads, then currents start to flow through each of the three branches. Nevertheless the conductance ratio of the two transversal branches is greatly affected by the position of the cross-junction. As can be observed from Figure 1, one of the two branches gets shorter as the other gets longer. If the transversal tube is not

ballistic then the currents will change their ratio accordingly, that is higher currents will flow through the shorter branches. Current imbalance can be measured with differential front-end electronics, yielding a measure of the cantilever's deflection, which is further multiplied with the spring constant of the system to obtain the applied force.

The junction's integrity is maintained mainly by van der Waals forces and additionally by hydrophobic-hydrophilic effects if the system is immersed. An off-plane force, i.e. a force along the y axis, could compromise the coupling of the tubes or even break them apart.

Basically the sensor is a molecular potentiometer whose actuation could be performed for instance by cell motility or by any other molecular phenomena. A sensor of this kind has the same functionality with a lateral force microscope. However it has the advantage of allowing massive parallelization.

### 3 MECHANICS OF NANOTUBES AND CELL MEMBRANES

Modeling the mechanics of the device was performed by using molecular dynamics and required the *ab initio* parameterization of the force-field in order to cope with the heterogeneity of a system including both carbon nanotubes and molecules. The cantilever's oscillation modes have been studied under perturbations induced by forces of tens of pN, a range compared for instance to those developed by cells during motility related processes.

We opted for the latter one as implemented in the freely-available program NAMD [3]. This force-field is faster than *ab initio* and semi-empirical methods allowing simulations with more than  $10^5$  atoms for time intervals of about 1ns. Compared with Brenner potentials that describe typically carbon-carbon interactions, the CHARMM force field was parameterized for a large spectrum of molecules, notably for amino-acids and phospholipids. This advantage becomes obvious when simulating the sensor, or just part of it, in contact with a cellular membrane.

#### 3.1 Ab initio force-field parameterization

Empirical force fields in CHARMM's class were previously used to model carbon-nanotubes [4] but their main task was to account for hydrophobic-hydrophilic effects somehow neglecting the mechanics of the tubes under important deformations. Accurate experimental information about Young's modulus and Poisson's ratio of carbon nanotubes is still missing from literature, besetting the parameterization procedure to rely on *ab initio* calculations. All quantum mechanical computations in this section were performed with Siesta [5], within the density functional theory (DFT).

The first set of simulations were conducted in order to obtain statistics on bond lengths, angles, Urey-Bradley (UB) and improper dihedrals values as required by CHARMM force field. This was achieved for three

different nanotubes, one armchair (5,5), one zig-zag (8,0) and one chiral (6,3) having approximately the same characteristic lengths. A variable-cell relaxation of the tubes, considered infinitely long, was performed subject to a convergence criteria of residual forces less than 0.01eV/Å. We used a LDA Hamiltonian, an integration grid cutoff of 60Ry, a double zeta (DZ) atomic orbital basis set with an energy shift of 160meV or equivalently a confinement/cutoff radius of 2.85Å. The final values for  $r_0$ ,  $\theta_0$ ,  $r_{0UB}$  and  $R_{vdW}$  are presented in Table 1.

k	189,580693	$r_0$	1,43257520454
$k_\theta$	115,723856	$\theta_0$	118,891824301
$k_{UB}$	22,699013	$r_{0UB}$	2,46731009022
<i>intra-tube</i>			
$\epsilon_{vdW}$	-0,105262	$R_{vdW}$	4,000000
<i>inter-tube</i>			
$\epsilon_{vdW}$	-0,070000	$R_{vdW}/2$	1,992400

Table 1: CHARMM force-field parameters

The second phase of the parameterization procedure consisted in fitting the spring constants  $k$ ,  $k_\theta$ ,  $k_{UB}$  and the Lennard-Jones well-depth  $\epsilon_{vdW}$  against energy versus strain curves as obtained with Siesta. Since our calculations are similar with those performed in Reference 6 and rely on the same code, we took into account their calculated Poisson's ratio of 0.14 when preparing strained tubes for relaxation. As opposed to the same reference we extended the study to strains in the range [-10,10]% with a step of 1%, in order to obtain well-behaved parameters even at large deformations. The system under study was a (5, 5), 5 cells long carbon nanotube. For each strain we took the already relaxed structure of this tube, modified its length to  $l_0(1+\Delta l/l_0)$  and radius to  $r_0(1-\nu\Delta l/l_0)$ , to accelerate the forthcoming relaxation. After constraining the boundary atoms in planes perpendicular to the tube's axis we re-minimize the energy.

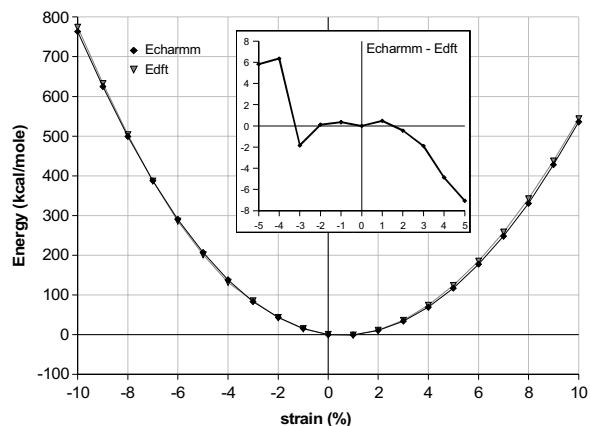


Figure 2: Energy vs. strain curves as obtained with Siesta and NAMD. The inset shows the error around the origin

To obtain positive spring constants and a negative well-depth we used Lagrange multipliers within the goal function, defined as the mean square of energy differences as calculated with Siesta and NAMD at different strains (see Figure 2), but not before shifting their energy minima to zero.

### 3.2 Force sensor simulation

In the first MD simulation, the cantilever measuring 36nm was pushed upon with a constant force of 10pN equally distributed between its ten terminal atoms while keeping the other end of the tube fixed.

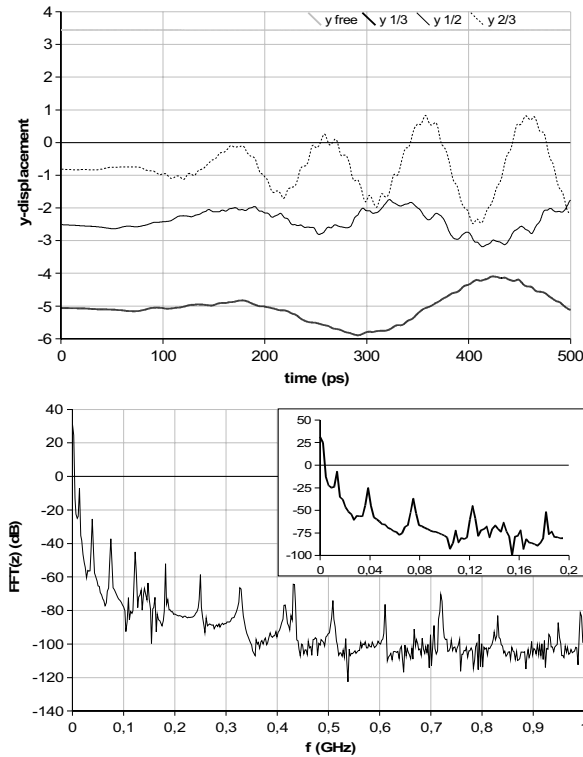


Figure 3: Displacement along y axis. (Bottom) Spectrum of the z deflection for one atom belonging to the sensor's tip

Turning on the force at the initial simulation time was similar to applying a step function stimulus, simultaneously exciting all the frequency modes of the system.

Three different positions of the (5,5) transverse tube, measuring 20 nm, were chosen to study the influence of the friction; at one third, at half and at two thirds from either edge of the cantilever. The simulation step was of 1fs, the total simulation time was of 0.5ns and proved to be sufficient for capturing at least one period of the cantilever's fundamental mode. A supplementary relaxation was performed before running the system in order to minimize the van der Waals interaction energy.

There should be in principle no important deflection along y since the applied force is constrained in the x-z plane. However Figure 3(top) revealed a different situation.

Even if initially constant, the cantilever's deflection starts to oscillate with increasing amplitude. A closer examination confirmed that the motion of the cantilever is stick-and-slip like due to rapid fluctuations in the van der Waals potential of the underlying tube. As we will see in the next section this spurious movement will greatly influence the charge transport through the junction as the latter is extremely sensitive to the inter-tube distance.

Heating is more pronounced with the transverse tube approaching the sensor's tip and it explains the smearing of the cantilever's spectrum observed in Figure 3(bottom). We plan further studies of this system in the presence of a Nose-Hoover thermostat that could minimize the artifacts induced by thermal effects.

## 4 SENSOR ELECTRONIC TRANSPORT

The transduction of the cantilever's deflection into an electrical signal has been investigated in the framework provided by Landauer-Buttiker theory with a tight-binding description of the system.

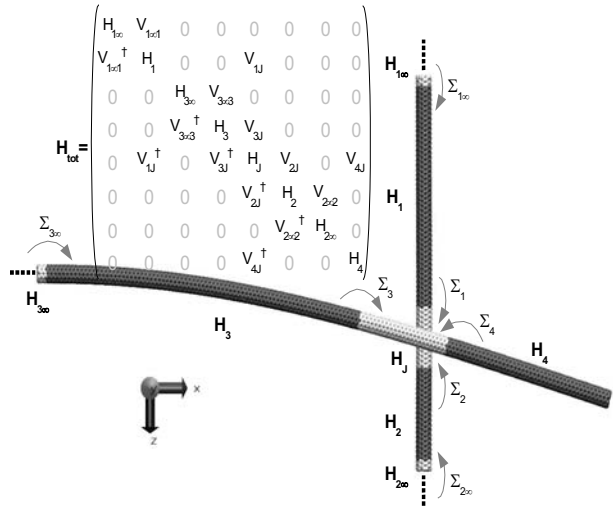


Figure 4: System's real-space partitioning and Hamiltonian.

Modeling the charge transport through the carbon-nanotube cross-junctions is a delicate task. Since the junction is maintained, by non-covalent bonding, it is relatively free to move in the x-z plane. Thus, thermal fluctuations of the junction's position will hugely influence the behavior of the device this effect to obtain the non-zero temperature behavior of this device and need to be addressed specifically.

### 4.1 Model description

The computation scheme is very similar with the one described in Reference 7. We used a Tight-Binding Hamiltonian including only  $\pi$  orbitals but as opposed to typical calculations we included the cosine factor like in the Slater-Koster scheme to account for the anisotropic inter-

tube coupling. An exponential decay was considered as well in order to limit the interaction range between non-covalently bonded atoms of the two distinct tubes.

Infinite pristine (5,5) CNTs were placed at the end of each the first three regions (denoted with  $H_{1...3}$ ) of the sensor's tubes to simulate the effect of electron reservoirs.

The transverse nanotube was "doped" by modifying the on-site energy  $\epsilon_0$  from zero to a random value equally distributed within  $[-1\text{eV}, 1\text{eV}]$ . Leads and the tubes they contact were set to an electrochemical potential of  $\pm 0.5\text{eV}$ .

In order to accelerate the computation of the Green's functions we partitioned the system like in Figure 4. After completing the Hamiltonian's matrix elements a fast, self-energy based elimination method was used to invert an otherwise large system matrix. Self-energies were propagated backwards from leads to junction as illustrated in the same figure. Practically one single large inversion was performed to invert for the junction Green's functions, corresponding to a Hamiltonian that is not too sparse as opposed to the other regions. We used the Fisher-Lee relation and the Landauer-Büttiker formula, as described in Reference 8 to obtain the interest, thermally-smearred conductances, i.e.  $G_{12}$ ,  $G_{13}$  and  $G_{23}$ .

## 4.2 Simulation results

Simulations at zero temperature with a longitudinal tube deflected in different positions showed that the device behaves non-monotonically. Universal conductance fluctuations play an important role, especially in the case of the sharp dopant distribution. Even more important are the atomic details of the cross-junction. Displacements as low as half an Angstrom give rise to important fluctuations in  $G_{13}$  and  $G_{23}$  as can be observed in Figure 5.

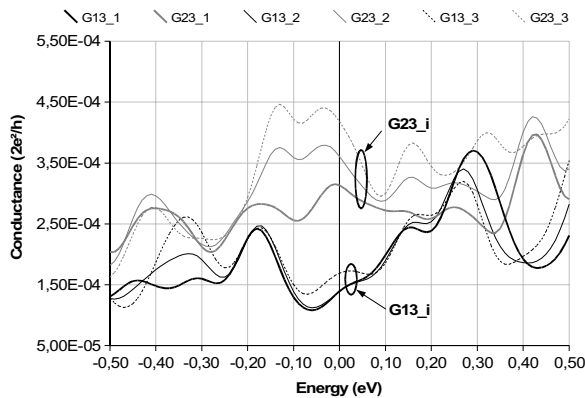


Figure 5: Smearred conductance between leads 3, 2 and 1 varies strongly at small perturbations of the cantilever.

Because relaxing the sensor in molecular dynamics is too slow to obtain enough intermediary positions of the cantilever, we took samples from the dynamical trajectory of the system as obtained in Section 3. Around a given junction position we took other twenty five closely located

sites. The length of the distribution interval was of  $\sim 2\text{\AA}$ , consistent with thermal displacement fluctuations as know from the classical cantilever theory.

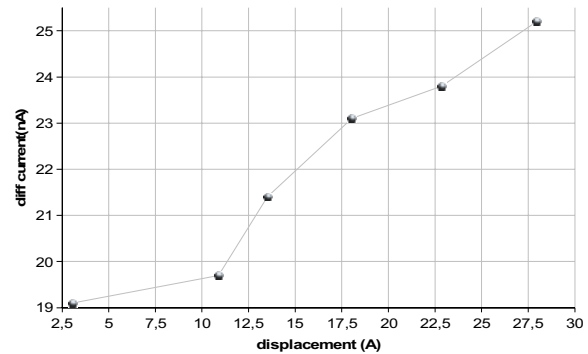


Figure 6: Deflection current dependence.

After computing the conductances and currents we convoluted the obtained values with a thermal-smearing function yielding the curve in Figure 6. This second smearing is considered here for to randomize the phase of electrons that tunnel through a fluctuating junction, and should not be confounded with the smearing applied to obtain the smooth conductance curves of Figure 5, accounting for the broadening of the Fermi-Dirac distribution with temperature.

## 5 CONCLUSIONS

After investigating the carbon nanotube-based device proposed in Section 2 by modeling phenomena characteristic to different scales we evaluate positively its suitability for measuring forces specific to the cellular scale. We note however several challenges posed by the coupling of phenomena belonging to different scales like the influence of the inter-tubes distance, typically modeled though molecular dynamics, and the variation of the currents computed though quantum transport calculations. Future work will have to take into account more thoroughly and systematically the influence of thermal noise on the functioning of the device.

## REFERENCES

- [1] G. della Torre et al., Nanotechnology 14, 765-771, 2003
- [2] M. Zheng et al., Science 302, 1545-1548, 2003
- [3] L. Kale et al., J. Comp. Phys. 151, 283-312, 1999
- [4] W.H. Noon et al., J.P. Ma. Chemical Physics Letters, 355, 445-448, 2002
- [5] J.M. Soler et al., Int. J. Quantum Chem. 65, 453, 1997
- [6] D.S. Portal et al., Phys. Rev. B 59, 12678, 1999
- [7] M.P. Anantram and T.R. Govindan, Phys. Rev. B 58, 4882, 1998
- [8] S. Datta, Cambridge University Press, 1995